REGULAR ARTICLE

Phosphorus speciation and bioavailability in diverse biochars

Terry J. Rose (ORCID) · **Cassandra Schefe · Zhe (Han) Weng · Michael T. Rose ·
Lukas van Zwieten · Lei Liu · Andrew L. Rose**

Abstract

Background and aims Erosion of phosphorus (P)-rich soil into waterways is a major contributor to eutrophication. To minimize the build-up of P in agricultural soils, greater knowledge of the bioavailability and fate of P from soil amendments is required.

Methods We used X-ray Absorption Near Edge Structure (XANES) spectroscopy to resolve the major P species in nine diverse biochars. We then examined the relationship between biochar P extracted using a range of typical soil (water, Bray2 and Colwell) and plant (2% citric acid, and 2% formic acid) assays. We compared these with ryegrass P uptake via bioassay.

Results Linear combination fitting indicated Al-phosphate (variscite) was the dominant P species in biochars derived from cattle feedlot manure, sugarcane trash and sugarcane bagasse, reflecting the likely Al content of the feedstock. Non-apatite Ca-phosphates (monocalcium phosphate or $CaHPO_4$) were the major P species in poultry litter, green waste, papermill sludge, wheat chaff, sugarcane mill mud and rice husk biochars. Biochar P was poorly water soluble but largely soluble in weak acids (formic and citric acids). Despite this, biochar P extracted by citric and formic acid was a poor predictor of P bioavailability to ryegrass, with the percentage of total P extracted by water

T. J. Rose · L. van Zwieten · L. Liu
Southern Cross Plant Science, Southern Cross University, PO Box 57, Lismore, NSW 2480, Australia

T. J. Rose (✉)
Centre for Organics Research, Southern Cross University, PO Box 57, Lismore, NSW 2480, Australia
e-mail: terry.rose@scu.edu.au

C. Schefe
Schefe Consulting, 59 Sheridan Court, Rutherglen, Vic 3685, Australia

Z. (. Weng · M. T. Rose · L. van Zwieten
NSW Department of Primary Industries, 1243 Bruxner Highway, Wollongbar, NSW 2477, Australia

A. L. Rose
School of Environment, Science and Engineering, Southern Cross University, PO Box 57, Lismore, NSW 2480, Australia

Present Address:
Z. (. Weng
Department of Animal, Plant and Soil Sciences, Centre for AgriBioscience, La Trobe University, Bundoora, Vic 3083, Australia

or by the Bray2 reagent providing the best prediction of ryegrass P uptake.

Conclusions The P in biochar was identified by XANES spectroscopy as predominantly Ca and/or Al-P. Water and Bray2 extraction provided the best predictors of plant available P from biochars in a plant bioassay.

Keywords Bioavailability · Biochar · Phosphorus · XANES

Introduction

Addition of phosphorus (P) to soils is essential to maintain current levels of global agricultural output due to widespread native deficiencies of P in soil (Batjes 1997) and continual P removal in harvested produce (Rose and Wissuwa 2012). However application of P in fertilizers, manures and other amendments is costly for farmers and presents an environmental hazard if this added P moves into waterways (Richardson et al. 2011). Indeed, the vast majority of non-point source P inputs to waterways arise from crop and pasture lands (Manuel 2014). Knowledge of P bioavailability in P-containing soil amendments, and understanding the fate of added P in the plant-soil system, is therefore crucial for the development of robust nutrient management strategies that maximize crop production while minimizing potential negative environmental impacts.

Biochar is a soil amendment that has attracted increasing interest over the past decade, having been shown to reduce N_2O emissions from soils (Cayuela et al. 2014), increase soil organic matter through direct input of C as well as stabilization of rhizodeposits (Weng et al. 2017), reduce contaminant availability (Kookana 2010; Park et al. 2011), and enhance crop P nutrition (Slavich et al. 2013; Van Zwieten et al. 2015). This enhanced P nutrition may occur indirectly because biochar can help overcome other soil constraints to enable plant roots to explore more soil, or it can increase soil pH, which consequently mobilizes P bound to Al- or Fe-(oxy)hydroxides in acidic soils (Van Zwieten et al. 2015). However, when feedstocks that contain substantial amounts of P are pyrolyzed, the resulting biochar can also act as a source of bioavailable P (Chan et al. 2008; Silber et al. 2010). The bioavailability of this P will in turn depend on its chemical speciation in the biochar.

Several recent studies have used solution-phase ^{31}P-nuclear magnetic resonance (NMR) spectroscopy to characterize P speciation in a range of pyrolyzed or hydrothermally treated manures and sewage sludges (Dai et al. 2015; Huang and Tang 2015; Qian and Jiang 2014; Uchimiya et al. 2015). Uchimiya et al. (2015) investigated P speciation in ash-rich biochars derived from manures, sewage sludge, and corn stover, and in low ash (2–5 wt%) pecan shell biochars, reporting the presence of Mg-orthophosphate (and struvite or whitlockite) in all biochars based on the strong (r = 0.98) correlation between the concentrations of P and Mg in NaOH-EDTA extracts. However, no spectral data supporting this conclusion were presented. In the same study, higher pyrolysis temperatures led to increasing amounts of orthophosphate in the NaOH-EDTA extracts of high-ash chars, similar to the observations of Qian and Jiang (2014). However, it is possible that the inorganic P quantified was an artifact of the extraction with NaOH-EDTA, since phosphate in the solid biochar is likely to be associated with a cation. Dai et al. (2015) suggested that much of the P present in cow manure biochar was present as apatite, but this was also speculative given that no definitive data were presented.

X-ray absorption near edge structure (XANES) spectroscopy has been used to characterize P speciation in biochar. An increasing proportion of apatite was detected at higher pyrolysis temperatures in biochars prepared from bone material (slaughterhouse waste) (Zwetsloot et al. 2015) and animal slurry and bone meal (Bruun et al. 2017). More recently, Robinson et al. (2018) investigated P speciation in a wide range of biochars and their feedstocks using XANES spectroscopy and found that hydroxyapatite was the dominant P form in the majority of biochars (all of which were produced at 480–500 °C), while pyrophosphate was also observed in some samples.

Despite the utility of XANES for identifying P speciation in biochars, a rapid, cheap and practical predictive assay is needed to determine P bioavailability in biochar. Several studies have examined the bioavailability of P in biochar-amended soils using diffusive gradient gels (DGT) (Bruun et al. 2017; Christel et al. 2016), but this technique is relatively time and labor intensive compared to simple wet chemistry methods. We are aware of only one study that has attempted to associate P bioavailability in biochars with a wet chemistry extraction assay, which found that P extraction with 2% formic acid provided the best prediction of P bioavailability in the biochar as assessed using a ryegrass

bioassay (Wang et al. 2012). However, this study only investigated high-P chars made from two feedstocks, and it is not known whether the results are relevant to biochars produced from a wider range of feedstocks.

The aim of the present study was therefore to resolve the P speciation in a diverse range of biochars (prepared using different feedstocks) using XANES spectroscopy and relate P extracted from the biochar using a range of wet chemical assays typically used for assessing P availability to P bioavailability based on a plant bioassay.

Materials and methods

Biochars

Nine biochars were previously produced from a range of feedstocks (poultry manure, green waste, cow manure, paper sludge, wheat chaff, sugarcane bagasse, sugarcane mill mud, sugarcane trash and rice husk) at pyrolysis temperatures ranging from 500 to 550 °C for use in a range of laboratory/glasshouse (Van Zwieten et al. 2010) and field studies (Rose et al. 2016; Slavich et al. 2013; Van Zwieten et al. 2013; Van Zwieten et al. 2015). All biochars were produced using slow pyrolysis with a minimum time at highest treatment temperature (HTT) of 30 min. These pyrolysis temperatures reflect those used in commercial slow pyrolysis technologies where syngas is the primary product. Samples used in this study were retrieved from archived samples that had been stored in sealed containers with minimal headspace at −18 °C, then ground and sieved to <1 mm for XANES analysis or < 2 mm for use in the chemical extraction and ryegrass P-uptake assays. Detailed physico-chemical characteristics of each biochar are given in Supplementary Tables S1-S3 in Electronic Supplementary Material.

P K-edges XANES

P K-edge XANES measurements were performed at the National Synchrotron Radiation Research Centre (NSRRC), Taiwan, using the tender XAS beamline 16A1. Photon energy was set using a fixed-exit double crystal Si(111) monochromator with vertically collimating pre-mirror and toroidal focusing mirrors and calibrated using the L_{III} edge of a Nb foil. Samples were analyzed in fluorescence mode using a Lytle detector. A varying step size was used to maximize data generation in regions of

interest (0.5 eV at 2103–2138 eV, 0.2 eV at 2138–2171 eV, 1.2 eV at 2171 eV and an increase in step size by 0.03 eV at every measurement through to 4.0 eV at 2445.2 eV). The beam spot size on the sample was ~0.5 × 0.4 mm, with dwell times of 2 s for the pre-edge and Extended X-ray Absorption Fine Structure (EXAFS) regions of the spectrum, and 3 s in the near edge region.

Biochar samples (ground and sieved to <1 mm) were mounted on a metal disc using double-sided Kapton polyimide tape. XANES spectra were also collected from a selection of calcium (Ca)-, potassium (K)-, sodium (Na)-, aluminum (Al)-, iron (Fe)- and organic P reference materials (Fig. S1). Three scans were performed on each sample, which were then averaged prior to analysis.

All spectra were normalized, aligned and calibrated using Athena-Demeter 0.9.25, as described in Ravel and Newville (Ravel and Newville 2005). As the unknown samples generally had a high signal-to-noise ratio, data were not smoothed. Likely P species in the biochar samples were determined by comparison with the spectra of reference materials (Supplementary Fig. S1) through a linear combination fitting (LCF) approach, using Athena (Ravel and Newville 2005). The weighting for each reference material was not constrained during the LCF procedure, nor was the sum of all the weights forced to equal one, as it is unlikely that the total P signal of the XANES spectrum is only comprised of the reference materials included. Goodness-of-fit was determined based on the least residual factor (R-factor).

Once a short-list of standards of interest were compiled using LCF, the relative importance of each reference material to the XANES spectrum for each sample was determined through sequential removal and addition of each standard from the LCF list, noting the change in the R-factor and spectral fit upon removal (termed ΔR), as described in Andersson et al. (2016). The standard which elicited the greatest change in the R-factor was determined to be of greatest importance in obtaining a good fit of the standards to the unknown spectra. The feasibility of these fits was also evaluated through visual assessments, based on the unique spectral features of each standard, and knowledge of the chemical composition of the biochar samples.

Chemical extractions of P from biochars

Biochar samples were extracted in triplicate with water (pH 7.0), 2% citric acid, 2% formic acid (Hedley and McLaughlin 2005), and based on the Bray 2 (Bray and

Kurtz 1945) and Colwell (Colwell 1963) procedures. Briefly, for the water, citric and formic acid extractions, samples were shaken in a 1:100 *w/v* biochar:solution ratio in an end-over-end shaker for 16 h, before being centrifuged at 25000 *x G* and the supernatant collected following filtration through a Whatman #4 filter paper. Orthophosphate concentration in the extracts was determined using the method of Murphy and Riley (Murphy and Riley 1962). For the Colwell extraction, samples were shaken with 0.5 M $NaHCO_3^-$ at pH 8.5 in a 1:100 *v/v* biochar:solution ratio for 16 h before being centrifuged and filtered as above. A 10 mL aliquot was neutralized using 1 M H_2SO_4 and allowed to settle overnight before P concentration was assessed as above. For the Bray 2 extraction, samples were shaken with 0.03 M NH_4F and 0.1 M HCl for 15 min, before being centrifuged at 25000 *x G* for 10 min. The supernatant was removed for analysis. Total P in the biochars was determined by digesting 0.2 g of biochar with 5 mL of aqua regia in a MARS microwave oven (CEM Corp., Matthews, NC, USA) and quantifying the P concentrations of the digest solution using inductively coupled plasma mass spectrometry (ICP-MS) (Perkin Elmer, Massachusetts, USA).

Plant bioassay

To investigate the plant bioavailability of P from biochars, a plant bioassay was conducted using perennial ryegrass (*Lolium perenne* L.) as the test crop. To minimize any indirect effects of biochar on soil P availability and plant growth (*e.g.* through changes in soil pH or provision of other nutrients that may be limiting) we used a neutral sandy soil (Arenosol; IUSS Working Group WRB 2014) with low native P levels and a low P buffering index. All other key plant nutrients were then added to the soil in excess to ensure that P was the only limiting nutrient. Chemical properties of the soil used are presented in Supplementary Table S4.

Free draining, 2 L black plastic pots were filled with 2 kg of air-dried soil. Basal nutrients (except P) were pipetted onto the surface of each pot as per Rose et al. (2007) and thoroughly mixed into the soil 24 h later. 1 kg of soil was then removed from each pot and biochar was thoroughly mixed at the necessary dose required to provide 50 mg total P kg^{-1} soil. Control pots either received 50 mg P in the top 1 kg of soil as water-soluble KH_2PO_4 (positive control) or nil P (negative control). Three replicate pots of all treatments were

prepared and laid out in a randomized block design in a temperature-controlled glasshouse at Southern Cross University, Lismore, NSW, Australia.

Ryegrass seeds were sown 5 mm deep at 25 seeds per pot on 22 July, 2014 and pots were watered to 70% field capacity. Seedlings were thinned to 15 plants per pot at 14 days after sowing (DAS). Ryegrass shoots were harvested at 27, 42, 56, 78, 96 and 110 DAS by cutting shoots approximately 10 mm from the soil surface. Nitrogen was added after each harvest as NH_4NO_3 (15 mg N kg^{-1} soil) in dilute solution. Shoot samples were dried at 60 °C for 5 d when constant weight was reached. After dry weights were recorded, shoots were finely ground and 0.2 g of subsample digested with 5 mL aqua regia, then the P concentration assayed by ICP-MS as above.

Statistical analysis

Data on cumulative biomass production and P accumulation in ryegrass shoots over six harvests were analyzed using a one-way analysis of variance fitting P amendment (nil-P, KH_2PO_4-P or one of nine biochars) in Genstat using a probability level of 0.05. Significance of differences between treatment means was tested using Duncan's multiple range test.

In order to visualize the relationships between biochar properties (total N, total C, CEC and lime equivalent [$CaCO_3$ equivalent] added per pot), extractable-P (water-, Colwell-, Bray2, Formic- and Citric-P) and P uptake by ryegrass, standardized principal components analysis was performed, using the "*vegan*" package (Oksanen et al. 2017) in R software (R Core Team 2013). Values were scaled to unit variance prior to PCA, and all values were greater than the limit of quantification. Correlations between individual biochar properties, extractable P measures and ryegrass P uptake are also presented in Supplementary Fig. 2. In addition, the first-derivative of the XANES spectra (2140–2180 eV) for each biochar were divided into 40 bins and pairwise correlations between each wavelength segment and total-P, extractable-P and P-uptake measures (as above) were assessed to explore relationships between P-speciation and P-availability. The first-derivative rather than the normalized spectra were used to provide higher resolution of smooth spectral features such as those associated with spectral shoulders. This was achieved using functions in the R packages

"*prospectr*" (Stevens and Ramirez-Lopez 2013) and "*gplots*" (Warnes et al. 2019).

Results

Phosphorus speciation in biochars

While total extractable P in the biochars (hot acid extract) ranged from 1.5 mg g^{-1} (rice husk biochar) to 32 mg g^{-1} (sugarcane mill mud biochar), the water-soluble P was an order of magnitude lower, ranging from 0.1 mg g^{-1} in sugarcane trash to 4.9 mg g^{-1} in poultry litter biochar (Table 1). Typical soil P extraction methods Colwell-P and Bray 2-P extracted from 2.4% (sugarcane bagasse) to 42% (cow manure) and 4.2% (bagasse) to 45% (rice husk) of the total P, respectively. Formic acid extracted 12% of total P in the sugarcane bagasse biochar and all of the P in the poultry litter biochar, while citric acid extracted 13% of total P in the sugarcane bagasse biochar and 92% of total P in the chicken manure biochar (Table 1).

XANES analysis showed the biochars to contain a mix of Ca, K, Na and Al phosphates. LCF further indicated that the P speciation of the biochars could be characterized as either Ca-dominant or Al-dominant

(Table 2). The Ca-dominant biochars were derived from wheat chaff, poultry litter, papermill sludge, rice husk, sugarcane mill mud and green waste. In comparison, the Al-dominant biochars were derived from cow manure, sugarcane trash and sugarcane bagasse. Of the Ca-dominant biochars, those derived from poultry litter and sugarcane mill mud showed strong, almost identical spectral features that clearly indicate the prominence of Ca-phosphates, notably a strong post-edge shoulder at 2148.7 eV (peak iii) and tertiary peak at 2156 eV (peak v) (Fig. 1). LCF results further indicate the importance of CaH_2PO_4 and $Ca_3(PO_4)_2$ in these two biochars, as demonstrated by the high ΔR values for the corresponding standards in the LCF (high ΔR means that removal from the LCF fit resulted in a large change in the R-factor) (Table 2). The high P concentration of these two biochars (2.1% w/w for poultry litter and 3.2% w/w for sugarcane mill mud; Table 1) contributed to a relatively high signal-to-noise ratio in these samples, enabling clear resolution of the spectral features observed.

The clarity of XANES spectral features for the other Ca-dominant biochars also correlated with the P content, as expected based on loss of resolution at low signal-to-noise ratios. The wheat chaff biochar (1.05% w/w P) also exhibited a shoulder feature related to calcium phosphates, but less prominently than in the

Table 1 Extractable P using different extraction methods from biochars from different source materials. Errors represent SEM ($n = 3$)

Biochar feedstock and highest treatment temperature	Phosphorus concentration (mg g^{-1}) and proportion of total extractable P (%) [a]					
	Water-P	Citrate-P	Formic-P	Colwell-P	Bray 2-P	Total P [b]
Cow manure 500 °C	1.0 ± 0.06 (14)	5.1 ± 0.07 (72)	4.0 ± 0.16 (56)	3.0 ± 0.02 (42)	1.4 ± 0.03 (20)	7.1
Wheat chaff 550 °C	2.2 ± 0.08 (21)	3.3 ± 0.17 (32)	3.6 ± 0.03 (34)	1.8 ± 0.03 (17)	3.1 ± 0.05 (30)	11
Poultry litter 550 °C	4.9 ± 0.21 (23)	19 ± 0.07 (92)	22 ± 0.23 (102)	8.2 ± 0.03 (39)	6.4 ± 0.10 (31)	21
Papermill sludge 500 °C	0.5 ± 0.02 (6.0)	5.4 ± 0.25 (67)	5.4 ± 0.23 (67)	1.6 ± 0.03 (20)	0.5 ± 0.02 (6.1)	8.1
Rice husk 500 °C	0.6 ± 0.04 (42)	0.8 ± 0.00 (54)	0.9 ± 0.02 (57)	0.6 ± 0.00 (40)	0.7 ± 0.03 (45)	1.5
Sugarcane trash 550 °C	0.1 ± 0.00 (5.7)	1.0 ± 0.08 (38)	1.2 ± 0.04 (45)	0.9 ± 0.00 (34)	0.3 ± 0.01 (11)	2.6
Sugarcane bagasse 550 °C	0.1 ± 0.01 (1.9)	0.4 ± 0.01 (13)	0.4 ± 0.01 (12)	0.1 ± 0.01 (2.4)	0.1 ± 0.00 (4.2)	3.1
Sugarcane mill mud 550 °C	0.1 ± 0.00 (0.21)	13 ± 0.06 (43)	14 ± 0.15 (43)	5.5 ± 0.07 (18)	2.1 ± 0.03 (6.6)	32
Green waste 550 °C	0.1 ± 0.00 (3.8)	1.0 ± 0.02 (43)	1.1 ± 0.02 (47)	0.3 ± 0.07 (15)	0.2 ± 0.00 (7.0)	2.4

[a] Proportion of total extractable P (%) shown in parentheses

[b] Total extractable P determined using a hot aqua regia digest. Only one sample digested so no standard error of mean available

Table 2 Major P species determined by linear combination fitting of XANES spectra of standards to XANES spectra of biochars from different source materials

Biochar source material	Order of Ranking [a]				R factor
	1	2	3	4	
Cow manure	variscite (0.09175)	NaH_2PO_4 (0.04944)	Na_3PO_4 (0.03891)	NaPyroP (0.01287)	0.00760
Wheat chaff	$Ca(H_2PO_4)_2$ (0.12582)	NaH_2PO_4 (0.01154)	K_2HPO_4 (0.00152)	$Ca_3(PO_4)_2$ (0.00049)	0.00426
Poultry litter	$Ca(H_2PO_4)_2$ (0.06811)	$Ca_3(PO_4)_2$ (0.01661)	$CaHPO_4$ (0.00734)	K_2HPO_4 (0.00020)	0.00422
Paper sludge	$Ca(H_2PO_4)_2$ (0.10430)	NaH_2PO_4 (0.00789)	$Ca_3(PO_4)_2$ (0.00713)	apatite (0.00661)	0.01346
Rice husk	$Ca(H_2PO_4)_2$ $_4$ (0.15837)	NaH_2PO_4 (0.00557)	KH_2PO_4 (0.00365)	K_2HPO_4 (0.00348)	0.01124
Sugarcane trash	variscite (0.09481)	NaPyroP (0.06290)	$Ca_3(PO_4)_2$ (0.03510)	b	0.04100
Sugarcane bagasse	variscite (0.06370)	Na_3PO_4 (0.04003)	NaH_2PO_4 (0.03597)	NaPyroP (0.01278)	0.00831
Sugarcane mill mud	$Ca(H_2PO_4)_2$ (0.03666)	$Ca_3(PO_4)_2$ (0.00311)	NaH_2PO_4 (0.00224)	apatite (0.00151)	0.00466
Green waste	$Ca(H_2PO_4)_2$ (0.03439)	$Ca_3(PO_4)_2$ (0.01247)	Na_3PO_4 (0.00723)	$FePO_4•4H_2O$ (0.00607)	0.00720

[a] Values in parentheses represent ΔR, i.e. the change in the R-value when that P species was excluded from the fit

[b] Only three components are presented for the Sugarcane trash as the inclusion of any standard as a fourth component increased the R factor and reduced the goodness of fit

poultry litter and sugarcane mill mud biochar samples due to the mix of Ca, Na and K compounds identified in the LCF. The XANES spectra of the remaining three Ca-dominant materials were increasingly noisy as the P concentration decreased in the order of papermill sludge (0.81% w/w), green waste (0.24% w/w) and rice husk (0.15% w/w), which was near the limit of detection by P K-edge XANES.
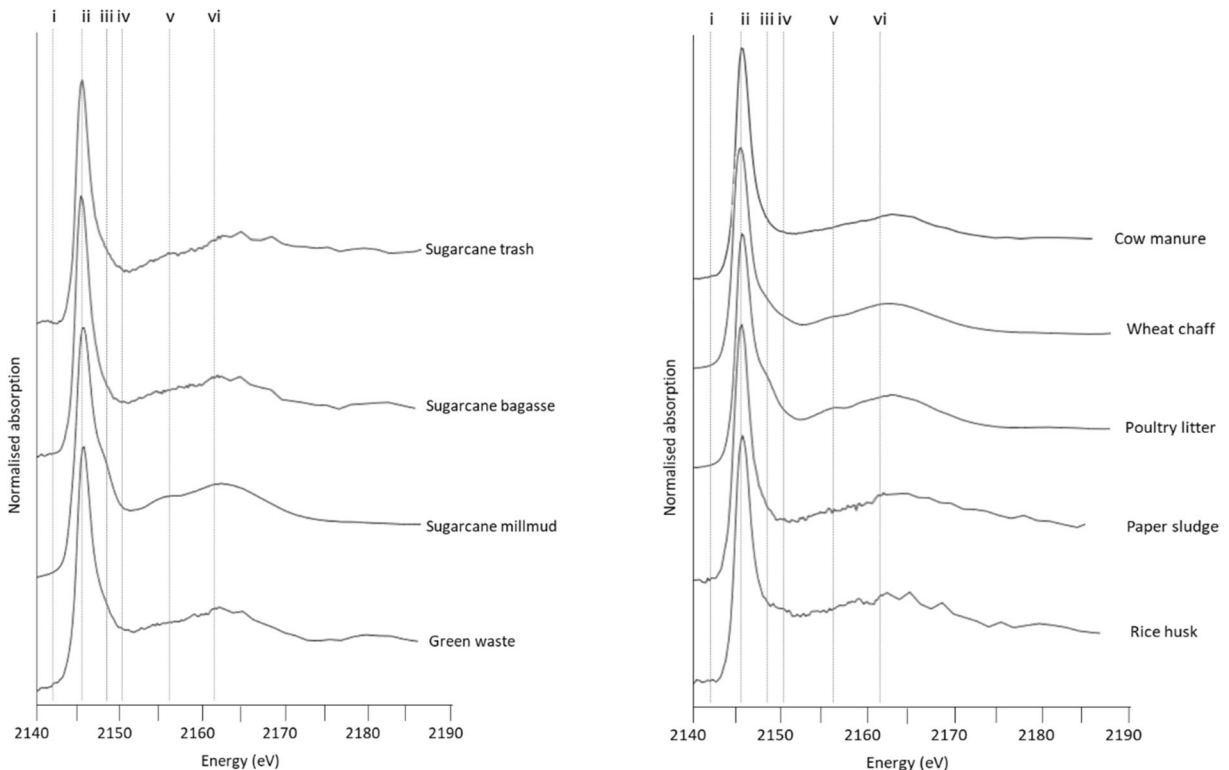
Fig. 1 Normalized P K-edge XANES spectra of biochars. Dashed lines indicate spectral features at i, 2143 eV (pre-edge), ii, 2146.5 eV (white line), iii, 2148.7 eV (shoulder), iv, 2151 eV (secondary shoulder peak), v, 2156 eV (tertiary peak), vi, 2162 eV (oscillation)

The other biochars (cow manure, sugarcane trash and sugarcane bagasse) were designated as Al-dominant due to the strong contribution of the variscite signal to the LCF. In the Ca-dominant samples, ΔR values for Ca-phosphates were much greater (sometimes by a factor of 10 or more) than ΔR values for the other compounds identified in the LCF. In contrast, for the Al-dominant biochars the difference in ΔR values between the first-ranked contributor (typically variscite) and second-ranked contributor to the LCF was quite small. More-over, as the key spectral characteristic of variscite is the absence of spectral features between the white line and the oscillation peak at 2162 eV, it could not be discounted that a range of compounds are contributing towards the spectrum, albeit at concentrations too low to exhibit clear spectral features. In addition, while the cow manure biochar (with 0.71% w/w P) showed a high signal-to-noise ratio, the sugarcane trash (0.26% w/w P) and sugarcane bagasse (0.31% w/w P) were nearing the limit of detection. Pyrophosphate was also detected in several of the biochars but was not the dominant P compound in any of these biochars (Table 2).

Phosphorus bioavailability to ryegrass plants

Biomass production in all biochar treatments was sig-nificantly ($p < 0.05$) higher than the nil P control except biochars derived from cow manure, papermill sludge and sugarcane mill mud (Fig. 2). Overall, however, ryegrass did not show a strong biomass response to P fertilization; the magnitude of differences was small, with cumulative biomass production after 110 d only 20% higher in the +P (KH_2PO_4) pots than the nil P control pots (Fig. 2a). In contrast, cumulative P accu-mulation in shoots of the +P plants was more than double that of the nil P plants (42 mg pot^{-1} vs 19 mg pot^{-1}), and there were significant ($p < 0.05$) differences in shoot P accumulation among biochar treatments (Fig. 2b). All biochar treatments and the positive control (+P) had significantly greater shoot P accumulation com-pared to the nil P control.

Ultimately, shoot P accumulation by ryegrass had the strongest association with the percentage of total P in biochars extracted by water or by the Bray2 extraction (Fig. 3). In contrast, neither the citric or formic acid extractable P, nor the % of total P extracted by 2% citric acid or formic acid, were strongly associated with shoot P accumulation in the ryegrass (Fig. 3). These results are supported by individual correlations between parameters,

where the only significant correlations ($P < 0.01$) were those between ryegrass P uptake and the % of total P extracted by water (r = 0.89) or Bray reagent (r = 0.93), the correlation between the % of total P extracted by water and Bray reagent (r = 0.98), and the correlation between the % of total P extracted by formic acid and citric acid (r = 0.95) (Supplementary Fig. 2). Furthermore, there was no significant correlation between XANES spectral fea-tures and P uptake by ryegrass plants, water-extractable P or Bray-extractable P. However, spectral features around 2151 and 2156 eV (the secondary and tertiary shoulder peaks, respectively) were correlated with Colwell-, citric- and formic-extractable P in biochars (Fig. 4). Higher P-availability with these extracts was associated with first-derivative spectra values closer to 0, indicative of shoul-ders at these regions.

Discussion

Phosphorus speciation in diverse biochars

The higher amounts of P extracted by citric and formic acid (Table 1) likely reflect their capacity to solubilize various Ca-phosphates, which were the dominant inor-ganic P species in most biochars (Table 2), and these data agree well with an earlier report that around 70% of the P in manure-derived biochars was extracted by 2% citric acid when they were produced at lower pyrolysis temperatures (Christel et al. 2014). However, Christel et al. (2014) also found that when biochars were pro-duced at temperatures at or above 600 °C the amount of P extracted by 2% citric acid was negligible. The strong prominence of Ca-phosphates has been reported in both plant-based and bio-waste-based biochars (Bruun et al. 2017; Robinson et al. 2018; Zwetsloot et al. 2015); however, the dominant form of Ca-phosphate observed in these earlier studies was apatite. While apatite was always considered in the initial group of standards for LCF in this study, inclusion of $Ca_3(PO_4)_2$ instead result-ed in a better fit. This was likely due to the slight reduction in the size of the tertiary peak at 2156 eV for $Ca_3(PO_4)_2$ compared to the more prominent peak at that energy for apatite. This may be attributable to the likely increased presence of apatite at higher pyrolysis temper-atures (Bruun et al. 2017) compared with the relatively low pyrolysis temperatures (500–550 °C) used to pre-pare the samples in this study (Supplementary Table S1).

a. Biomass accumulation

b. Phosphorus accumulation
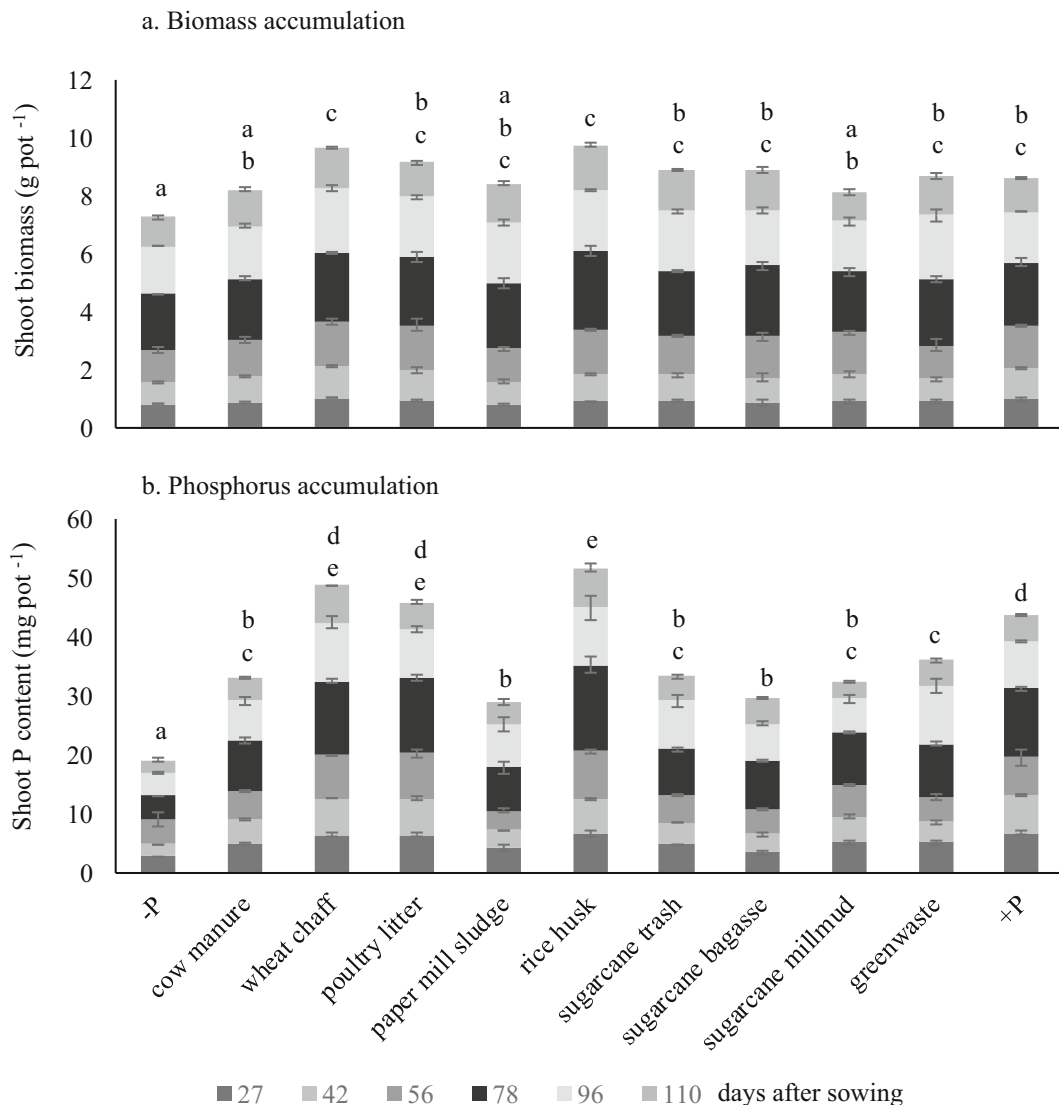
Fig. 2 (**a**) Biomass accumulation and (**b**) P accumulation in shoots of ryegrass grown in the glasshouse harvested at 27, 42, 56, 78, 96 and 110 days after sowing. Bars that do not share a common letter are significantly different at $P = 0.05$. "-P" refers to the nil added P control treatment, while "+P" refers to the treatment with added KH_2PO_4. Error bars represent standard error of the mean (n = 3)

We are not aware of any reports that suggest a strong presence of Al-phosphates in biochars, but Seiter et al. (Seiter et al. 2008) used XANES and sequential extraction to demonstrate that poultry litter amended with alum (aluminum sulfate) exhibited a higher proportion of Al-bound P species than raw poultry litter, which had a higher proportion of Ca-P minerals. The presence of Al in the cattle feedlot manure may be a result of the management, movement and collection of the feedlot manure waste prior to biochar production, where soil could be picked up and mixed into the manure. Sweeten

et al. (1986) analysed the ash content of feedlot manures showing that they were dominated by silica (ranging from between 53 and 60% by weight), but also contained a considerable Al content, analysed at between 7.8 and 9.8% of the ash content (w/w). Thus the Al content of the feedstock may have led to preferential formation of Al-P species over Ca-P species in the resulting biochar. The formation of Al-P in the sugarcane trash and bagasse biochars reflects the herbage Al content of sugarcane biomass (Watt 2003). It should also be noted that the poorer quality of XANES spectra for

Fig. 3 Principal components analysis of biochar properties in relation to P uptake. Abbreviations are as follows: CM = cow manure, WC = wheat chaff, PL = poultry litter, PS = paper sludge, RH = rice husk, ST = sugarcane trash, SB = sugarcane bagasse, SM = sugarcane mill mud, GW = greenwaste, CEC = cation exchange capacity, Lime equiv. = Lime (CaCO$_3$) equivalents
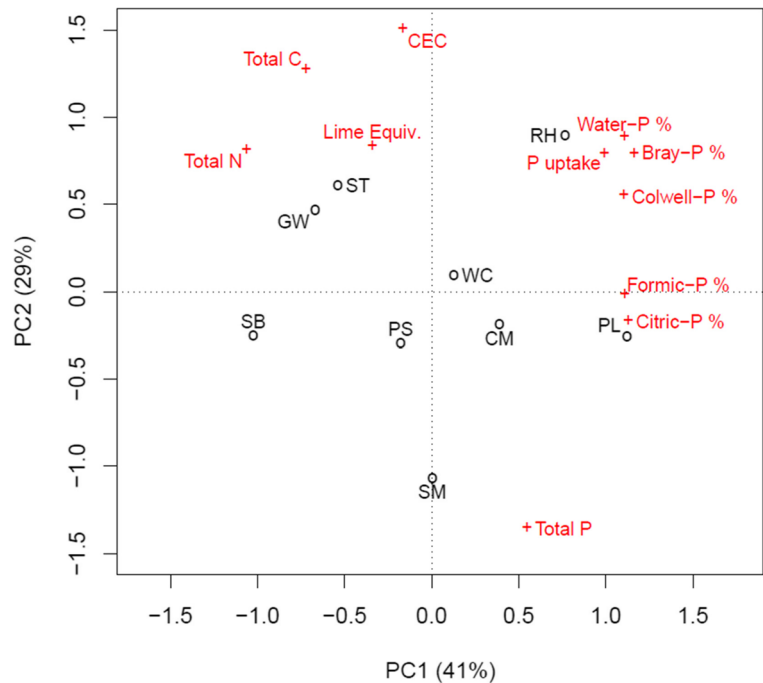
the sugarcane trash and sugarcane bagasse biochars (due to low P content) may have influenced the reliability LCF results for these samples. That the sugarcane mill-mud biochar is dominated by Ca-P species reflects the processing of sugarcane juice, which utilizes lime and/or calcium hydroxide as a clarification agent to flocculate inorganic P and other impurities (Doherty et al. 2002).

LCF additionally identified the presence of pyrophosphate in several of the biochars, even though pyrophosphate may not have been present in the original (non-pyrolyzed) material. An earlier XANES study similarly identified the presence of pyrophosphate in several biochars but not in their raw feedstock material (Robinson et al. 2018), leading to the conclusion that it was likely to have been produced during the pyrolysis process, potentially through the transformation of phytic acids or polyphosphates in the feedstocks. While Na pyrophosphate was the only pyrophosphate standard used in our study, it is possible that pyrophosphates of other cations, such as Ca may be present.

Phosphorus bioavailability to ryegrass plants

Biochar can impact on a range of soil properties including pH, soil C, cation exchange capacity, and bulk density (Quin et al. 2014; Van Zwieten et al. 2015), which may improve overall root and plant growth,

leading to further plant P uptake. We aimed to assess the potential bioavailability of P within the various biochars, and therefore attempted to minimize the influence of the indirect impacts of biochar on soil P cycling in our ryegrass bioassay by using a near-neutral sandy soil low in available and total P (see key soil chemical properties in Table S4), by providing all other nutrients in adequate amounts, and by using small (2 L) pots to minimize feedback effects of differences in root growth. This was largely successful, because the amount of C added to the soil in biochar and the liming capacity of the biochar were not strongly associated with shoot P accumulation of ryegrass after 6 harvests (Fig. 3). Thus, we presume that the P accumulated in the ryegrass shoots largely reflected the bioavailability of P in the biochar, although the possibility of specific biochar-induced short-term phytotoxicity can't be eliminated (Rombolà et al. 2015).

The lack of a strong association between formic acid extractable P and ryegrass P accumulation contrasts findings from an earlier study that found extraction with 2% formic acid provided the best prediction of P bioavailability in high-ash biochars based on a ryegrass bioassay (Wang et al. 2012). The reason for this discrepancy may be due to the fact that we assessed biochars made from a diverse range of feedstocks, while Wang et al. (2012) investigated bioavailability in biochars
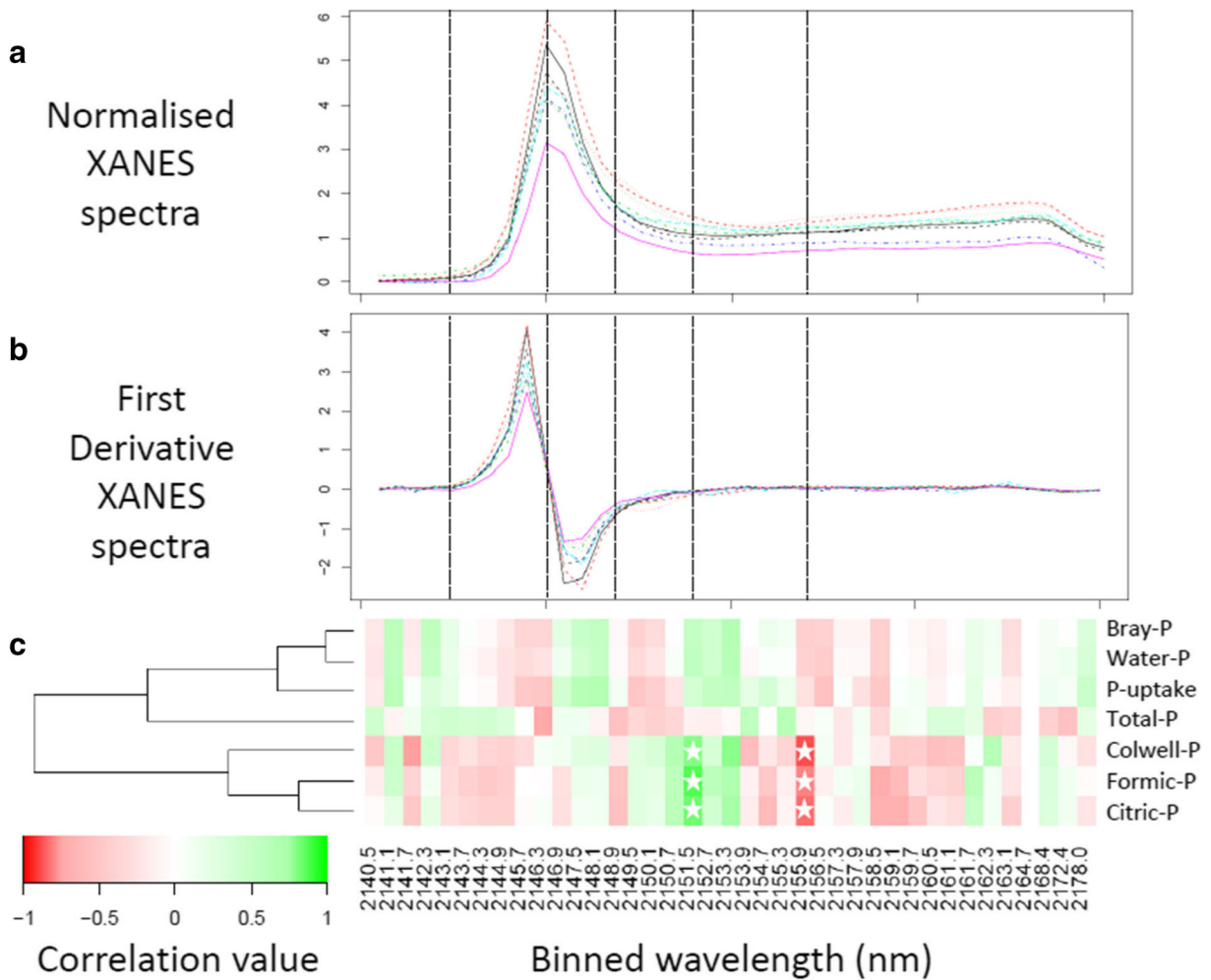
Fig. 4 Relationships between XANES spectra and measures of P-availability and uptake from a diverse range of biochars ($n = 9$). Normalized P K-edge XANES spectra of biochars (**a**) and their first-derivatives (**b**) were averaged over 40 bins across the 2140–2180 eV region. The heatmap (**c**) displays colour-coded correlation co-efficients for measures of P-availability and uptake against first-derivative XANES spectral regions. Stars in a cell correspond to a significant correlation ($P < 0.05$). Vertical dashed lines show spectral features as described in Fig. 1

made from two feedstocks with four pyrolysis temperatures. A further difference between the studies is that we applied biochars at rates to equalize the amount of P added to each pot, while Wang et al. (2012) added the same mass of biochar to pots, so pots received different amounts of P. Wang et al. (2012) also included rock phosphate and superphosphate P treatments and fitted a Mitscherlich function to the combined data of ryegrass P uptake from biochar, superphosphate and rock phosphate. Closer inspection of the data in Wang et al. (2012) suggests that the apatite and superphosphate data are strong contributors to the shape of the fitted curve, and may have contributed to the conclusion that 2% formic acid was a good predictor of P bioavailability

in the biochars. However, we also note that a sonification step was included in the extraction methods of Wang et al. (2012) and this may also have contributed to the discrepancy in results.

Our direct analysis of the XANES spectra with measures of P-availability and uptake from biochars suggests that simplified indicators of P-speciation, represented by individual (non-interacting) regions of XANES spectra, cannot accurately predict plant P-uptake. In contrast, the significant association between certain measures of P availability (citric-, formic- and Colwell-P) and specific regions of the XANES spectra are indicative of, but not exclusive to Ca-P species. This highlights the promise of this technique for obtaining

information regarding the influence of P-speciation on P-availability. However, it is likely that information on P-speciation alone will not be sufficient for a complete assessment of biological P availability, considering the additional importance of other physicochemical properties of biochar, such as particle size/surface area, acid neutralizing capacity or potentially stimulatory/ inhibitory organic compounds. Regardless, the use of a greater number of diverse biochars to enable more comprehensive multivariate statistical predictions would help to improve on the current limitations in this study, where only nine biochars were assessed.

Conclusion

The study indicated that non-apatite Ca-phosphates (monocalcium phosphate or $CaHPO_4$) were the major P species in most biochars while Al-phosphates were dominant in biochars derived from cow manure, sugarcane trash and sugarcane bagasse feedstocks. Biochar P was poorly water soluble but largely soluble in weak acids (formic and citric acids); however, P extracted by the weak acids was not correlated with P uptake by ryegrass plants. While our results indicated that the percentage of total P extracted by water or by the Bray2 extraction provided the best predictor of ryegrass P uptake, further research with a wider range of biochars (different feedstock and pyrolysis temperature) is necessary to determine whether these extractants can be used to determine P fertiliser value.

Author contributions   The manuscript was written through contributions of all authors. All authors have given approval to the final version of the manuscript.

References

Andersson KO, Tighe MK, Guppy CN, Milham PJ, McLaren TI, Schefe CR, Lombi E (2016) XANES demonstrates the release of calcium phosphates from alkaline vertisols to moderately acidified solution. Environmental Science & Technology 50: 4229–4237. https://doi.org/10.1021/acs.est.5b04814

Batjes NH (1997) A world dataset of derived soil properties by FAO–UNESCO soil unit for global modelling. Soil Use Manag 13:9–16. https://doi.org/10.1111/j.1475-2743.1997.tb00550.x

Bray RH, Kurtz LT (1945) Determination of total, organic, and available forms of phosphorus in soils. Soil Sci 59:39–46

Bruun S, Harmer SL, Bekiaris G, Christel W, Zuin L, Hu Y, Jensen LS, Lombi E (2017) The effect of different pyrolysis temperatures on the speciation and availability in soil of P in biochar produced from the solid fraction of manure. Chemosphere 169: 377–386. https://doi.org/10.1016/j.chemosphere.2016.11.058

Cayuela ML, van Zwieten L, Singh BP, Jeffery S, Roig A, Sánchez-Monedero MA (2014) Biochar's role in mitigating soil nitrous oxide emissions: a review and meta-analysis. Agric Ecosyst Environ 191:5–16. https://doi.org/10.1016/j.agee.2013.10.009

Chan KY, Van Zwieten L, Meszaros I, Downie A, Joseph S (2008) Using poultry litter biochars as soil amendments. Soil Research 46:437–444. https://doi.org/10.1071/SR08036

Christel W, Bruun S, Magid J, Jensen LS (2014) Phosphorus availability from the solid fraction of pig slurry is altered by composting or thermal treatment. Bioresour Technol 169: 543–551. https://doi.org/10.1016/j.biortech.2014.07.030

Christel W, Bruun S, Magid J, Kwapinski W, Jensen LS (2016) Pig slurry acidification, separation technology and thermal conversion affect phosphorus availability in soil amended with the derived solid fractions, chars or ashes. Plant Soil 401:93–107. https://doi.org/10.1007/s11104-015-2519-0

Colwell J (1963) The estimation of the phosphorus fertilizer requirements of wheat in southern New South Wales by soil analysis. Aust J Exp Agric 3:190–197. https://doi.org/10.1071/EA9630190

Doherty WOS, Greenwood J, Pilaski D, Wright PG (2002) The effect of liming conditions in juice clarification. Proceedings of the Australian Society of Sugar Cane Technology, Vol. 24

Dai L, Tan F, Wu B, He M, Wang W, Tang X, Hu Q, Zhang M (2015) Immobilization of phosphorus in cow manure during hydrothermal carbonization. J Environ Manag 157:49–53. https://doi.org/10.1016/j.jenvman.2015.04.009

Hedley M, McLaughlin M (2005) Reactions of phosphate fertilizers and by-products in soils. In: JT Sims, AN Sharpley (eds) phosphorus: agriculture and the environment. American Society of Agronomy, crop science Society of America, and soil science Society of America, Madison, WI

Huang R, Tang Y (2015) Speciation dynamics of phosphorus during (hydro)thermal treatments of sewage sludge. Environmental Science & Technology 49:14466–14474. https://doi.org/10.1021/acs.est.5b04140

IUSS Working Group WRB (2014) World Reference Base for soil resources 2014. International soil classification system for naming soils and creating legends for soil maps (3rd ed.). FAO, Rome, ISBN 978-92-5-108370-3

Kookana RS (2010) The role of biochar in modifying the environmental fate, bioavailability, and efficacy of pesticides in soils: a review. Soil Research 48:627–637. https://doi.org/10.1071/SR10007

Manuel J (2014) Nutrient pollution: a persistent threat to waterways. Environ Health Perspect 122:A304–A309. https://doi.org/10.1289/ehp.122-A304

Murphy J, Riley JP (1962) A modified single solution method for the determination of phosphate in natural waters. Anal Chim

Acta 27:31–36. https://doi.org/10.1016/S0003-2670(00)88444-5

Oksanen J, Blanchet FG, Friendly M, Kindt R, Legendre P, McGlin D, Minchin P, O'Hara RB, Simpson G, Solymos P, others (2017) vegan: Community Ecology Package. R package version 2.4–3. 2017 [accessed 2016 Jan 1]. R package version 2.4–3. 2017 edn

Park JH, Choppala GK, Bolan NS, Chung JW, Chuasavathi T (2011) Biochar reduces the bioavailability and phytotoxicity of heavy metals. Plant Soil 348:439–451. https://doi.org/10.1007/s11104-011-0948-y

Qian T-T, Jiang H (2014) Migration of phosphorus in sewage sludge during different thermal treatment processes. ACS Sustain Chem Eng 2:1411–1419. https://doi.org/10.1021/sc400476j

Quin PR, Cowie AL, Flavel RJ, Keen BP, Macdonald LM, Morris SG, Singh BP, Young IM, Van Zwieten L (2014) Oil mallee biochar improves soil structural properties - a study with x-ray micro-CT. Agric Ecosyst Environ 191:142–149. https://doi.org/10.1016/j.agee.2014.03.022

R Core Team (2013) R: a language and environment for statistical computing. R Foundation for Statistical Computing, Vienna, Australia

Ravel B, Newville M (2005) ATHENA, ARTEMIS, HEPHAESTUS: data analysis for X-ray absorption spectroscopy using IFEFFIT. J Synchrotron Radiat 12:537–541. https://doi.org/10.1107/S0909049505012719

Richardson AE, Lynch JP, Ryan PR, Delhaize E, Smith FA, Smith SE, Harvey PR, Ryan MH, Veneklaas EJ, Lambers H, Oberson A, Culvenor RA, Simpson RJ (2011) Plant and microbial strategies to improve the phosphorus efficiency of agriculture. Plant Soil 349:121–156. https://doi.org/10.1007/s11104-011-0950-4

Robinson JS, Baumann K, Hu Y, Hagemann P, Kebelmann L, Leinweber P (2018) Phosphorus transformations in plant-based and bio-waste materials induced by pyrolysis. Ambio 47:73–82. https://doi.org/10.1007/s13280-017-0990-y

Rombolà AG, Marisi G, Torri C, Fabbri D, Buscaroli A, Ghidotti M, Hornung A (2015) Relationships between chemical characteristics and phytotoxicity of biochar from poultry litter pyrolysis. J Agric Food Chem 63:6660–6667. https://doi.org/10.1021/acs.jafc.5b01540

Rose T, Wissuwa M (2012) Rethinking internal phosphorus utilization efficiency: a new approach is needed to improve PUE in grain crops. In: Sparks DL (ed) Advances in agronomy. Academic Press, Burlington

Rose TJ, Keen B, Morris SG, Quin P, Rust J, Kearney L, Kimber S, Van Zwieten L (2016) Application of woody biochar and woody mulch to mitigate nitrous oxide emissions from a poultry litter-amended soil in the subtropics. Agric Ecosyst Environ 228:1–8. https://doi.org/10.1016/j.agee.2016.05.004

Rose TJ, Rengel Z, Ma Q, Bowden JW (2007) Differential accumulation patterns of phosphorus and potassium by canola cultivars compared to wheat. J Plant Nutr Soil Sci 170:404–411. https://doi.org/10.1002/jpln.200625163

Seiter JM, Staats-Borda KE, Ginder-Vogel M, Sparks DL (2008) XANES spectroscopic analysis of phosphorus speciation in alum-amended poultry litter. J Environ Qual 37:477–485. https://doi.org/10.2134/jeq2007.0285

Silber A, Levkovitch I, Graber ER (2010) pH-dependent mineral release and surface properties of cornstraw biochar:

agronomic implications. Environmental Science & Technology 44:9318–9323. https://doi.org/10.1021/es101283d

Slavich PG, Sinclair K, Morris SG, Kimber SWL, Downie A, Van Zwieten L (2013) Contrasting effects of manure and green waste biochars on the properties of an acidic ferralsol and productivity of a subtropical pasture. Plant Soil 366:213–227. https://doi.org/10.1007/s11104-012-1412-3

Stevens A, Ramirez-Lopez L (2013) An introduction to the prospectr package. R package Vignette R package version 0.1.3

Sweeten JM, Korenberg J, LePori WA, Annamalai K, Parnell CB (1986) Combustion of cattle feedlot manure for energy production. Energy in Agriculture 5:55–72

Uchimiya M, Hiradate S, Antal MJ (2015) Dissolved phosphorus speciation of flash carbonization, slow pyrolysis, and fast pyrolysis biochars. ACS Sustain Chem Eng 3:1642–1649. https://doi.org/10.1021/acssuschemeng.5b00336

Van Zwieten L, Kimber S, Morris S, Downie A, Berger E, Rust J, Scheer C (2010) Influence of biochars on flux of N_2O and CO_2 from ferrosol. Soil Research 48:555–568. https://doi.org/10.1071/SR10004

Van Zwieten L, Kimber SWL, Morris SG, Singh BP, Grace PR, Scheer C, Rust J, Downie AE, Cowie AL (2013) Pyrolysing poultry litter reduces N_2O and CO_2 fluxes. Sci Total Environ 465:279–287. https://doi.org/10.1016/j.scitotenv.2013.02.054

Van Zwieten L, Rose T, Herridge D, Kimber S, Rust J, Cowie A, Morris S (2015) Enhanced biological N_2 fixation and yield of faba bean (Vicia faba L.) in an acid soil following biochar addition: dissection of causal mechanisms. Plant Soil 395:7–20. https://doi.org/10.1007/s11104-015-2427-3

Wang T, Camps-Arbestain M, Hedley M, Bishop P (2012) Predicting phosphorus bioavailability from high-ash biochars. Plant Soil 357:173–187. https://doi.org/10.1007/s11104-012-1131-9

Warnes GR, Bolker B, Bonebakker L, Gentleman R, Huber W, Liaw A, Lumley T, Maechler M, Magnusson A, Moeller S, Schwartz M, Venables B (2019) gplots: Various R Programming Tools for Plotting Data. R package version 3.0.1.1. https://CRAN.R-project.org/package=gplots. Accessed 27 Jan 2019

Watt DA (2003) Aluminium-responsive genes in sugarcane: identification and analysis of expression under oxidative stress. J Exp Bot 54(385):1163–1174

Weng Z, Van Zwieten L, Singh BP, Tavakkoli E, Joseph S, Macdonald LM, Rose TJ, Rose MT, Kimber SWL, Morris S, Cozzolino D, Araujo JR, Archanjo BS, Cowie A (2017) Biochar built soil carbon over a decade by stabilizing rhizodeposits. Nat Clim Chang 7:371–376. https://doi.org/10.1038/nclimate3276

Zwetsloot MJ, Lehmann J, Solomon D (2015) Recycling slaughterhouse waste into fertilizer: how do pyrolysis temperature and biomass additions affect phosphorus availability and chemistry? J Sci Food Agric 95:281–288. https://doi.org/10.1002/jsfa.6716